

# Coulomb implosion mechanism of negative ion acceleration in laser plasmas

T. Nakamura\*, Y. Fukuda, A. Yogo, M. Tampo, M. Kando, Y. Hayashi, T. Kameshima, A. S. Pirozhkov, T. Zh. Esirkepov, T. A. Pikuz, A. Ya. Faenov, H. Daido, and S. V. Bulanov

(Dated: March 8, 2022)

## Abstract

Coulomb implosion mechanism of the negatively charged ion acceleration in laser plasmas is proposed. When a cluster target is irradiated by an intense laser pulse and the Coulomb explosion of positively charged ions occurs, the negative ions are accelerated inward. The maximum energy of negative ions is several times lower than that of positive ions. The theoretical description and Particle-in-Cell simulation of the Coulomb implosion mechanism and the evidence of the negative ion acceleration in the experiments on the high intensity laser pulse interaction with the cluster targets are presented.

Recent developments in the ultra-intense laser pulse technology resulted in the intensity at the level above  $10^{22}$  W/cm<sup>2</sup> [1]. The ultra-intense laser pulse interaction with matter opens such new research fields as the fast ignition of inertial thermonuclear fusion [2], the charged particle beam acceleration for medical applications [3], and the development of compact sources of high energy electrons, ions and photons [4, 5, 6] (see also the review article [7] and literature quoted in).

The negative ion generation has attracted a great deal of attention due to various applications as the beam injectors for magnetically confined fusion devices [8], as the heavy ion fusion drivers [9], and for utilizing them in large scale ion accelerators [10]. Negatively charged ion beams are typically generated via the charge exchange process during the positive ion propagation through the alkali metal vapor. However, since the charge exchange cross section rapidly decreases as the incident energy exceeds keV level, it has been an important issue to find an effective way to generate the high energy negative ions. Laser plasma provides a source of the negative ions with the energy in keV~MeV range [11, 12, 13]. In the experiment presented in Ref. [11], the negative ions with the energy about MeV have been observed when the water droplets are irradiated by the ultra-short and ultra-intense laser pulse (40 fs,  $I \approx 10^{19}$  W/cm<sup>2</sup>). The negative ions were generated inside the laser plasma and are accelerated together with the positive ions. As far as it concerns the positive ion acceleration in the laser plasmas, there were invoked several mechanisms including the sheath acceleration [14], the Coulomb explosion [15], the shock acceleration [16], the radiation pressure dominant acceleration [17], the “after-burner” [18], etc. On the other hand, the acceleration mechanism of negative ions, according to our knowledge, has not yet been studied so far.

In the present Letter we propose the Coulomb implosion mechanism of the negative ion acceleration. When a cluster target is irradiated by an intense laser pulse and the ponderomotive pressure of the laser light blows away the electrons, the repelling force of an uncompensated electric charge of positive ions causes the cluster Coulomb explosion. In the case of a multi-species cluster with a relatively small number of the negative ions, where possible mechanisms of negative ion creation are discussed in Ref.[19], the electric field formed by the positively charged component accelerates the negative ions inward. The negative ions leave the target, passing through the center or bouncing its vicinity. Below we formulate the theoretical description and present the results of the Particle-in-Cell simulation

of the Coulomb explosion/implosion of a multi-species cluster. The evidence of the negative ion acceleration in the experiments on the high intensity laser pulse interaction with the cluster targets is presented as well.

At first, we consider the Coulomb explosion dynamics of a multi-species cluster. The cluster comprises the positive and negative ion components. Within the framework of hydrodynamics description the positive and negative ion motion is governed by the continuity equations:  $\partial_t n_{\pm} + \nabla \cdot (n_{\pm} \mathbf{v}_{\pm}) = 0$ , the Euler equations:  $\partial_t \mathbf{v}_{\pm} + (\mathbf{v}_{\pm} \nabla) \mathbf{v}_{\pm} = \pm e_{\pm} \mathbf{E} / M_{\pm}$ , and by the equation for the electric field:  $\nabla \cdot \mathbf{E} = 4\pi \sum (\pm e_{\pm} n_{\pm})$ . Here  $\mathbf{E}$  is the electric field, the subscript  $(\pm)$  stands for positive and negative ions,  $n_{\pm}$ ,  $\mathbf{v}_{\pm}$ ,  $\pm e_{\pm}$ , and  $M_{\pm}$  are their density, velocity, electric charge and mass. These equations admit a self-similar solution with homogeneous deformation, for which the densities are homogeneous,  $n_{\pm} = n_{\pm}(t)$ , and the velocities and electric field are linear functions of the coordinates:  $v_{i,\pm} = \dot{m}_{ik,\pm}(t) (m_{kj,\pm})^{-1}(t) x_j$ ,  $E_i = \epsilon_{ij}(t) x_j$ . Here summation over repeated indices is assumed. The matrix  $m_{ik,\pm}$  is the deformation matrix,  $\dot{m}_{ik,\pm}$  is its time derivative and  $(m_{kj,\pm})^{-1}$  is its inverse matrix (see Ref. [20]). Now we assume a spherical, cylindrical or planar symmetry of the flow, for which the deformation matrix has a diagonal form with equal diagonal elements,  $k_{\pm}(t)$ . In this case, the velocity of Lagrange element is given by  $v_{\pm} = \dot{k}_{\pm} x^0$  and of the Euler element by  $v_{\pm} = \dot{k}_{\pm} x / k_{\pm}$ , and the density is  $n_{\pm} = n_{0,\pm} / k_{\pm}^d$ , with  $n_{0,+}$  and  $n_{0,-}$  being the initial values of densities of the positive and negative ions;  $d$  equals to the dimension such that  $d = 1$ ,  $d = 2$  and  $d = 3$  correspond to planar, cylindrical, and spherical geometry, respectively. Substituting these functions to the above written equations, we obtain for  $k_{\pm}(t)$  a system of two nonlinear ordinary differential equations:

$$\frac{d^2 k_+}{dt^2} = \frac{\omega_+^2}{k_+^{(d-1)}} - \frac{\omega_{\pm}^2 k_+}{k_+^d}, \quad (1)$$

$$\frac{d^2 k_-}{dt^2} = \frac{\omega_-^2}{k_-^{(d-1)}} - \frac{\omega_{\mp}^2 k_-}{k_-^d}, \quad (2)$$

where we introduced  $\omega_+ = \sqrt{4\pi n_{0,+} e_+^2 / M_+}$ ,  $\omega_- = \sqrt{4\pi n_{0,-} e_-^2 / M_-}$ ,  $\omega_{\pm} = \sqrt{4\pi n_{0,-} e_+ e_- / M_+}$ , and  $\omega_{\mp} = \sqrt{4\pi n_{0,+} e_+ e_- / M_-}$ .

If the density of negative ions is small enough,  $n_{0,-} \ll e_+ n_{0,+} / e_-$ , then we assume it vanishes,  $n_{0,-} = 0$ , at the first step of approximation with respect to a small parameter  $e_- n_{0,-} / e_+ n_{0,+}$ . In this case for  $d = 3$ , Eq. (1) describes the Coulomb explosion of a positively charged cluster [21]. For initial conditions,  $k_+(0) = 1$  and  $dk_+/dt(0) = 0$ , its solution reads

$\sqrt{k_+(k_+ - 1)} + \log\left(\sqrt{k_+} + \sqrt{k_+ - 1}\right) = \sqrt{2}\omega_+t$ . In the case of cylindrical geometry,  $d = 2$ , which may correspond to the Coulomb explosion of the self-focusing channel [22], Eq. (1) yields  $\text{Erfi}\left(\sqrt{\log k_+}\right) = \sqrt{2/\pi}\omega_+t$ . Here  $\text{Erfi}(z) = \text{erf}(iz)/i$  is the complex error function which is a real function of its argument. In a planar geometry,  $d = 1$ , we have  $k_+ = 1 + (\omega_+t)^2/2$ .

Then, assuming the dependence of  $k_+$  on time to be given by the above written expressions, we obtain from Eq. (2) the equation  $d^2k_-/dt^2 + \Omega_-^2(t)k_- = \omega_-^2/k_-^{(d-1)}$  with  $\Omega_-(t) = \omega_{\mp}/(k_+(t))^{d/2}$  and with initial conditions  $k_-(0) = 1$  and  $dk_-/dt(0) = 0$ . If  $\omega_-/\Omega_- \ll 1$ , the negative ions during the first step move towards the center from where they bounce and move outwards. The ion velocity can be estimated to depend on the initial position,  $x^0$ , as  $|v_-| = \left(\int_0^\infty \Omega_-(t')dt'\right)x^0$ . In the opposite limit, when  $\omega_-/\Omega_- \gg 1$ , we seek a solution in the form of slowly varying and fast oscillating components,  $k_-(t) = K_-(t) + \tilde{k}_-(t)$ , with  $\langle \tilde{k}_- \rangle = 0$ , where  $\langle \dots \rangle$  denotes a time averaging. The component  $K_-$  corresponds to the equilibrium solution of Eq. (2) for frozen dependence on time of  $k_+$ , i.e.  $K_-(t) = (\omega_-/\omega_{\mp})^{2/d}k_+(t)$ . For oscillating component,  $\tilde{k}_-$ , we find the equation of an oscillator with a time dependent frequency:  $d^2k_-/dt^2 + d\Omega_-^2(t)k_- = 0$ . Due to a smallness of the ratio  $\omega_-/\omega_{\mp} \ll 1$  a dependence on time of  $\Omega_-(t)$  is slow and we can use the WKB approximation. This yields the expression for the oscillating part of  $k_-(t)$ . It reads  $\tilde{k}_-(t) = [k_+(t)]^{d/4} \cos\left(\sqrt{d} \int_0^t \Omega_-(t')dt'\right)$ , which describes the particle oscillations with growing amplitude and decreasing frequency.

The ion energy spectrum can be found by considering a dependence of the velocity on the ion initial position. We see that the ion kinetic energy,  $\mathcal{E} = M_-v_-^2/2$ , is proportional to the square of the ion initial coordinate:  $\mathcal{E} \propto (x^0)^2$ . Using a condition of the continuity in the phase space,  $dN_- = 4\pi n_{0,-}(x^0)^{d-1}d\mathcal{E}/|d\mathcal{E}/dx^0|$  we find that the ion energy spectrum is inversely proportional to the square root of energy,  $dN/d\mathcal{E} \propto 1/\sqrt{\mathcal{E}}$  in the case of planar geometry; it is flat,  $dN/d\mathcal{E} = \text{constant}$  in cylindrical geometry, and is proportional to the square root of energy  $\propto \sqrt{\mathcal{E}}$  in the case of spherical geometry. The negative ion energy is in a factor  $\kappa = (\omega_-/\omega_{\mp})^{4/d} = (e_-n_{0,-}/e_+n_{0,+})^{2/d}$  smaller than the energy of the positive ions.

Now we demonstrate the implosion dynamics of negative ions by using the two-dimensional Particle-in-Cell (PIC) simulations. The simulation conditions are as follows. The target is a cluster with the diameter of  $1 \mu\text{m}$  composed of electrons, protons and negative hydrogen ( $H^-$ ) ions whose densities are  $1.0n_c$ ,  $1.1n_c$ , and  $0.1n_c$ , respectively. Here

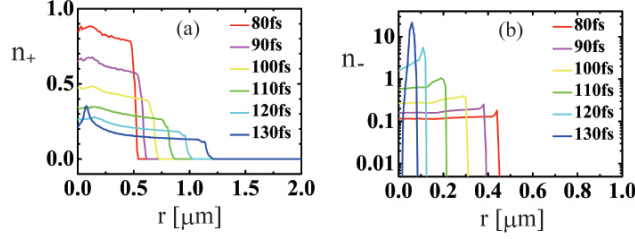


FIG. 1: Radial density profiles of (a) protons and (b) negative hydrogen,  $H^-$ , ions during the Coulomb explosion and implosion. The densities are normalized on the critical density.

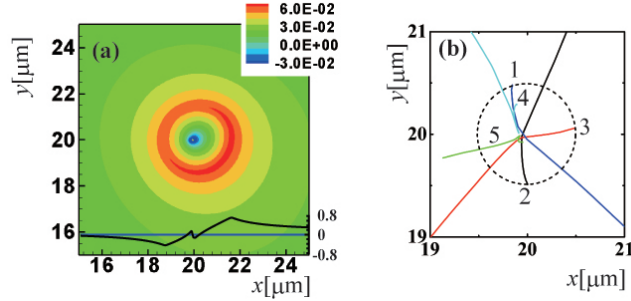


FIG. 2: (a) Distribution of the radial component of electric field  $E_r$  at time  $t=130$  fs. The electric field is normalized on the incident laser electric field, which is  $27\text{TV/m}$  in our simulations. The profile of  $E_r$  along the horizontal line passing  $y=20$  is shown in the lower part. (b) Trajectories of  $H^-$  ions.

$n_c = m_e \omega^2 / 4\pi e^2$  is the critical density for the laser light with the frequency  $\omega$ . In this case the parameter  $\kappa$  equals 0.1. The electron initial temperature is set to be equal to 500 eV. The ions are assumed to be initially cold. The target is located at the center of the simulation box which has a size of  $40\mu\text{m}$  in both the  $x$ - and  $y$ -directions. The laser pulse irradiates the target from the left hand side boundary. It propagates in the  $x$ - direction and is polarized along the  $y$ - direction. The pulse has a flat top form rising up in a laser period and keeping its peak intensity of  $1.0 \times 10^{20} \text{ W/cm}^2$  which is constant for the duration of 15 fs, where laser wavelength is  $1 \mu\text{m}$ . The laser pulse is focused to the spot with the diameter of  $3\mu\text{m}$  (FWHM), where the focal point is  $x = 18\mu\text{m}$ . The simulation box has  $4000 \times 4000$  meshes, with  $\simeq 1 \times 10^6$  quasi-particles used.

By the irradiation of the ultra-intense laser pulse, the electrons are heated and swept away from the target leaving the target positively charged. This results in the Coulomb explosion of the positive ions and in the Coulomb implosion for the negative ions. The time

history of radial density profile of protons and  $H^-$  ions along x-axis ( $x \leq 20$ ) is plotted in Fig. 1 (a) and (b), respectively ( $r = -x+20$ ). The protons expand radially due to the Coulomb explosion, having a rather flat distribution as in the self-similar solution of two-dimensional case.  $H^-$  ions start to move inward from the outer region, and they are most compressed at  $t = 130$  fs whose center is located at  $(x,y)=(19.95,20.0)$ , which is  $0.05 \mu\text{m}$  left to the target center. This off-center of the implosion comes from the asymmetry of laser irradiation. As the  $H^-$  ions are accelerated towards the center, the electric field, which sign is opposite to that of the outer region, is induced at the center due to accumulation of the negative charges, as it is seen in Fig.2 (a). The electric field decelerates the imploding  $H^-$  ions and attract protons towards the center which is seen in Fig.1(a). The trajectories of  $H^-$  ions are shown in Fig.2(b). Particles with numbers from 1 to 3 are initially located at the periphery of the target. They are accelerated towards the center and slightly deflected by the electric field and leave the target. They have maximum energy of 1 MeV when they reach the cluster center, and then they are gradually decelerated while leaving the target. Particle number 4 moves towards the center and then is reflected back by the induced strong electric field. Its energy at the time when it has left the target is 0.1 MeV. Particle number 5 being located near the center bounces between the outer and inner regions and then leaves the target. It achieves the energy being only  $\sim 30$  eV. As a result, energetic  $H^-$  ions are generated from the periphery of the target.

The Coulomb explosion/implosion of positive/negative ions is illustrated in Fig. 3, where the phase planes  $(y, p_y)$  are plotted. In the row (a,b) we show the ion phase planes at time  $t=80$  fs. We see the linear (self-similar) dependence of the ion momentum on the coordinate corresponding to the positive ion expansion and to the negative ion collapse. In the row (c,d) we plot the phase planes at the time  $t=180$  fs, after the negative ions have bounced from the central region. We see that both the positive and negative ions expand radially. A local compression of the positive ions induced by the electric field formed at the center is also seen in Fig. 3c.

The energy spectra of protons and  $H^-$  ions are shown in Figs.4(a) and (b), respectively. The spectra of protons are flat, which is in agreement with the theoretical prediction in the case of two-dimensional Coulomb explosion. The maximum energy of negative hydrogen  $H^-$  is equal to 1.0 MeV. We see that the negative ion energy is approximately ten times less than the energy of positive ions. This is in agreement with the above formulated theoretical

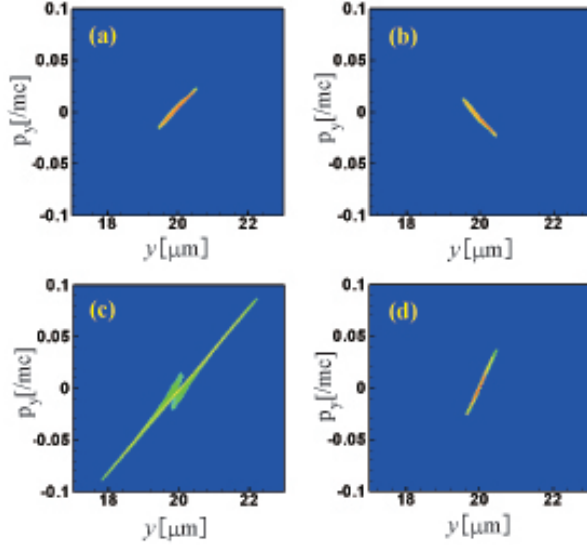


FIG. 3: Phase planes  $(y, p_y)$  of the positive (in the frames (a) and (c)) and negative (in the frames (b) and (d)) ions. The rows (a,b) and (c,d) correspond to the time  $t=80\text{fs}$  and  $t=180\text{fs}$ , respectively.

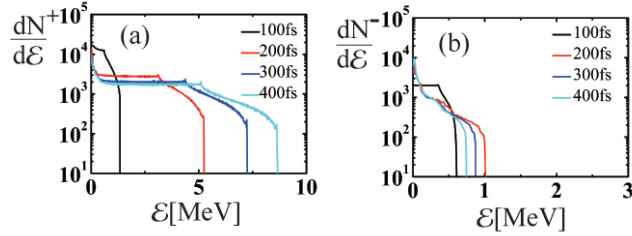


FIG. 4: Time history of the energy spectra of (a) protons, and (b)  $H^-$  ions.

model with  $\mathcal{E}_- = \kappa\mathcal{E}_+$ , for the parameter  $\kappa$  equal to 0.1 in our simulations.

In the case of lower values of the laser intensity or/and higher values of total initial number of the ions, the laser light does not blow away all the electrons. For example, when a laser intensity is  $I = 1.0 \times 10^{19}\text{W}/\text{cm}^2$  and a target has the same parameters as above calculations, we do not have a regime of pure Coulomb explosion. Nevertheless, the negative ions are accelerated towards the target center. Since the sheath field inside the expansion front is weakened by the bulk electrons, the energy achieved by negative ions does not oscillate and they sustain the energy after leaving the target.

Negative ions are observed in experiments using water droplet[11], or thin foil target[12]. In our experiments negative ions are observed for the first time using mixtures of  $\text{CO}_2$

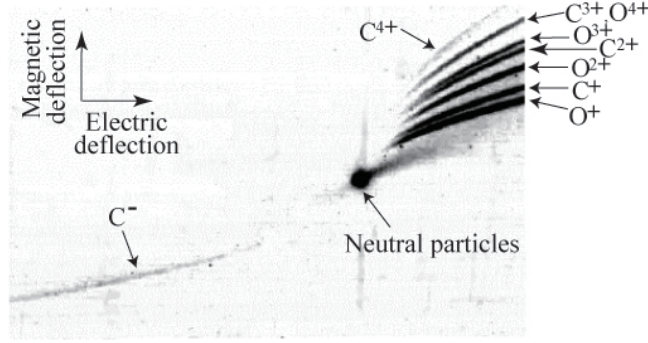


FIG. 5: A pattern registered on CR-39 with the Thomson parabola.

clusters and He gas target. The laser has energy of 130 mJ with pulse duration of 35 fs. The pulse is focused into the spot with 30  $\mu\text{m}$  in diameter, resulting in the intensity of  $7 \times 10^{17}$  W/cm<sup>2</sup> in vacuum. The CO<sub>2</sub> clusters with the diameters equal to 0.35  $\mu\text{m}$ , which contain  $5 \times 10^8$  molecules each, are generated using specially designed supersonic gas jet nozzle[23]. Average distance between the clusters is 5  $\mu\text{m}$ . The laser pulse contrast of  $10^{-6}$  at the ns time scale is expected to lead to the cluster heating and evaporation by the pre-pulse. This results in the interaction of the main, fs, laser pulse with the plasma clouds of larger volume and lower density than in the initial clusters. The registered parabolic line of the positive and negative ions accelerated in the Coulomb explosion/implosion are shown in Fig.5. The Thomson parabola is positioned in the direction of 135° from the laser axis, i.e. we observe the ions moving in the backward-aside direction with respect to the laser beam propagation. In Fig.5 we see the parabolic lines produced by negative C<sup>-</sup> ions as well as the carbon ions up to C<sup>4+</sup> ion and by the oxygen ions up to O<sup>4+</sup> ions. The maximum energy of positive C<sup>4+</sup> ions is 4.8 MeV, and that of the negative C<sup>-</sup> ions is 0.6 MeV. The ratio of maximum energy of positive and negative ions is 1/8, which corresponds to  $\kappa = 1/8$  with  $n_{0,-}/n_{0,+} \simeq 0.02$ . The detailed discussion of experimental results will be presented in the forthcoming papers [13].

In conclusion, the proposed Coulomb implosion model explains the acceleration of negatively charged ions in the laser-plasma. The negative ions initially located at the target periphery are accelerated more efficiently. A final energy of the negative ions is several times less than the positive ion energy. The Coulomb implosion mechanism is clearly demonstrated by the PIC simulations. Acceleration of positive ions via the Coulomb explosion is a well-known mechanism. Negative ions can be accelerated in the same field, however, their

acceleration occurs in the opposite direction with the bouncing-back in the vicinity of the center of symmetry, which results in the generation of high energy negative ions. We note here that the mechanism is applicable in the case of thin foil, self-focusing channel, and cluster according to in 1D, 2D, and 3D configuration.

We acknowledge a partial support from special Coordination Funds for Promoting Science and Technology commissioned by MEXT of Japan. The simulations are performed by using Altix3700 at JAEA Tokai.

\* E-mail address : nakamura.tatsufumi@jaea.go.jp

- 
- [1] V. Yanovsky, *et.al.*, Optics Express **16**, 2109 (2008).
  - [2] M.Tabak, *et.al.*, Phys. Plasmas **1**, 1626 (1994); M. Roth, *et.al.*, Phys. Rev. Lett. **86**, 436 (2001).
  - [3] I. Spencer, *et.al.*, Nucl. Instrum. Methods Phys. Res., Sect. B **183**, 449 (2001); S. V. Bulanov and V. S. Khoroshkov, Plasma Phys. Rep. **28**, 453 (2002); T. Toncian, *et.al.*, Science **312**, 410 (2006).
  - [4] W. P. Leemans, *et al.*, Nature Phys. **2** 696 (2006); S. Karsch, *et al.*, New J. Phys. **9**, 415 (2007).
  - [5] J. Denavit, Phys. Rev. Lett., **69**, 3052 (1992); A. Maksimchuk, *et al.*, *ibid.* **84**, 4108 (2000); E. L. Clark, *et al.*, *ibid.* **84**, 6703 (2000); R. A. Snavely, *et al.*, *ibid.* **85**, 2945 (2000); S. Hatchett, *et.al.*, Phys. Plasmas **7**, 2076 (2000); K. Matsukado, *et al.*, Phys. Rev. Lett. **91**, 215001 (2003); J. Fuchs, *et.al.*, Nature Phys. **2**, 48 (2006); C. Schwoerer, *et al.*, Nature (London) **439**, 445 (2006); M. Borghesi, *et al.*, Fusion Sci. Technol. **49**, 412 (2006); L. Willingale, *et al.*, Phys. Rev. Lett. **98**, 049504 (2007); A. Yogo, *et al.*, Phys. Rev. E **77**, 016401 (2008); T. Nakamura, *et al.*, *ibid.* **77**, 036407 (2008).
  - [6] J. D. Kmetec, *et al.*, Phys. Rev. Lett. **68**, 1527 (1992); S. V. Bulanov, *et al.*, *ibid.* **91**, 085001 (2003); K. Ta Phouc, *et.al.*, *ibid.* **91**, 195001 (2003); M. Kando, *et al.*, *ibid.* **99**, 135001 (2007); A. S. Pirozhkov, *et al.*, Phys. Plasmas **14**, 123106 (2007); A. Giulietti, *et al.*, Phys. Rev. Lett. **101**, 105002 (2008).
  - [7] G. Mourou, *et al.*, Rev. Mod. Phys. **78**, 309 (2006).
  - [8] T. Inoue, *et.al.*, Fusion Eng. Des. **56 – 57**, 517 (2001).

- [9] L. R. Grisham, Nucl. Instr. and Meth. A **464**, 315 (2001).
- [10] M. P. Stockli, Proceedings of LINAC 2006, pp.213 (2006).
- [11] S. Ter-Avetisyan, *et.al.*, J. Phys. B **37**, 3633 (2004).
- [12] R.V.Volkov, *et.al.*, JETP Lett. **76**, 139 (2002).
- [13] Y.Fukuda, A.Yogo, *et.al.*, in preparation.
- [14] A. V. Gurevich, *et al.*, Sov. Phys. JETP **22**, 449 (1966); S. J. Gitomer, *et al.*, Phys. Fluids **29**, 2679 (1986); P. Mora, Phys. Rev. Lett. **90**, 185002 (2003); M. Passoni and M. Lontano, *ibid.* **101**, 115001 (2008) .
- [15] T.Ditmire, *et.al.*, Nature (London) **386**, 54 (1997); K. Nishihara, *et al.*, Nucl. Instrum. Methods Phys. Res., Sect. A **464**, 98 (2001).
- [16] L.O.Silva, *et.al.*, Phys. Rev. Lett. **92**, 015002 (2004); M.S.Wei, *et.al.*, *ibid.* **93**, 155003 (2004).
- [17] T. Zh. Esirkepov, *et.al.*, Phys. Rev. Lett. **92**, 175003 (2004); F. Pegoraro and S. V. Bulanov, *ibid.* **99**, 065002 (2007) S. Kar, *et al.*, *ibid.* **100**, 225004 (2008).
- [18] L.Yin, *et. al.*, Phys. Plasmas **14**, 056706 (2007).
- [19] B. M. Smirnov, *Negative ions* (New York, McGraw-Hill, 1992).
- [20] L. I. Sedov, *Similarity and dimensional methods in mechanics* (CRC Press, 1993); S. V. Bulanov and M. A. Ol'shanetskij, Sov. J. Plasma Phys. **11**, 425 (1985).
- [21] I. Last, *et al.*, J. Chem. Phys. **107**, 6685.(1997).
- [22] G. S. Sarkisov, *et al.*, Phys. Rev. E **59**, 7042 (1999).
- [23] Y. Fukuda, *et al.*, Appl. Phys. Lett. **92**, 121110 (2008).